The Journal of Chemical Physics

Simulations of electrolyte between charged metal surfaces

Cite as: J. Chem. Phys. **153**, 044121 (2020); https://doi.org/10.1063/5.0012073
Submitted: 27 April 2020 . Accepted: 06 July 2020 . Published Online: 28 July 2020

Rodrigo Mór Malossi, Matheus Girotto, Alexandre P. dos Santos, and Yan Levin

The Journal of Chemical Physics ARTICLE scitation.org/journal/jcp

Simulations of electrolyte between charged metal surfaces

Cite as: J. Chem. Phys. 153, 044121 (2020); doi: 10.1063/5.0012073
Submitted: 27 April 2020 • Accepted: 6 July 2020 •
Published Online: 28 July 2020

Rodrigo Mór Malossi,[1] Matheus Girotto,[2] Alexandre P. dos Santos,[1] and Yan Levin[1,a)]

AFFILIATIONS

[1] Instituto de Física, Universidade Federal do Rio Grande do Sul, Caixa Postal 15051, 91501-970 Porto Alegre, RS, Brazil
[2] Instituto de Fisica, Universidade de Sao Paulo, Rua do Matao, 1371, 05508-090 Sao Paulo, SP, Brazil

[a)] **Author to whom correspondence should be addressed:** levin@if.ufrgs.br

ABSTRACT

We present a new method for simulating ungrounded charged metal slabs inside an electrolyte solution. The ions are free to move between the interior and exterior regions of the slab–electrolyte system. This leads to polarization of both sides of each slab, with a distinct surface charge induced on each surface. Our simulation method is based on the exact solution of the Poisson equation using periodic Green functions. To efficiently perform the calculations, we decouple the electrostatic energy due to surface polarization from that of purely Coulomb interaction between the ions. This allows us to combine a fast 3D Ewald summation technique with an equally fast calculation of polarization. As a demonstration of the method, we calculate ionic density profiles inside an electrolyte solution and explore charge neutrality violation in between charged metal slabs.

I. INTRODUCTION

Metal nanoparticles have attracted a lot of attention due to their many possible applications,[1–5] one of which is drug delivery.[6,7] To understand the interactions between the metal nanoparticles and stability of suspensions containing such particles, a variety of simulation methods have been developed.[8–12] Unfortunately, due to particle polarizability, the simulation methods are difficult to implement and require a lot of CPU time, thus limiting their practical use. Theoretical and simulation approaches were also developed in order to elucidate polarization effects in dielectrics.[13–20] Recently, it was theoretically predicted that like-charged spherical metal nanoparticles can attract each other inside an electrolyte solution.[5] The theoretical approach was based on the mean-field Poisson–Boltzmann (PB) theory, which is valid only for solutions containing a 1:1 electrolyte. If one wants to explore the interaction between nanoparticles in solutions containing multivalent ions, one needs to go beyond the simple PB theory. Unfortunately, at the moment, there are no reliable theoretical methods that can be used to study the interaction between metal nanoparticles in solutions containing a multivalent electrolyte. Simulations provide a viable alternative. However, even for two nanoparticles inside an electrolyte solution, such simulations are very involved. An alternative is to consider two metal slabs and then to appeal to the Derjaguin approximation to account for the curvature of particle surfaces. It is, therefore, the goal of the present paper to develop a simulation method that will allow us to calculate the ionic distribution in an electrolyte solution containing two parallel metal slabs.

This paper is organized as follows: we first calculate a closed form electrostatic potential for different regions of the electrolyte with parallel *grounded* metal slabs. We then extend this solution to slabs that are *not* grounded and that carry a net surface charge. Following this, we perform NVT Monte Carlo simulations to obtain ionic density profiles inside the electrolyte solution and explore charge neutrality violation between the metal slabs.

II. METHOD

If an ion is confined between grounded metal surfaces, the electrostatic potential can be calculated using the method of image charges. The difficulty is that one needs an infinite number of image charges for each ion. This substantially slows down the simulations, since large sums must be performed. A number of methods were

proposed to address this difficulty. Some approaches use a brute force sum of image charges, and others use a minimization procedure to calculate the induced charge on the surfaces,[15,21–24] which is then used to obtain the electrostatic potential. Unfortunately, there is an intrinsic slowness to both methods. A possible alternative is to model a metal surface using parameterized Lennard-Jones potentials.[25,26]

The fundamental difficulty of simulating systems with long range interaction is that the electrostatic potential cannot be cut off. This prevents one from using simple periodic boundary conditions that are standard for systems with short range forces. Instead, the simulation box must be periodically replicated so that the electrostatic potential inside the simulation cell results not only from the ions inside the cell but also from their infinite replicas. In the case of homogeneous electrolytes, summation over the replicas can be efficiently performed using Ewald techniques. The situation, however, becomes significantly more complex if one attempts to simulate the system with dielectric or metal interfaces. In recent papers,[27–29] the authors proposed the use of periodic Green functions to simulate electrolytes confined by dielectric surfaces or metal electrodes. The advantage of this method is that the polarization contribution to the electrostatic energy can be decoupled from the direct Coulomb interaction between the ions. The direct interaction can then be efficiently calculated using a modified 3D Ewald summation method, while the polarization contribution is calculated using fast converging sums obtained from the Green functions. Furthermore, for grounded metal surfaces, it is possible to analytically calculate the induced surface charge. This makes the method of periodic Green functions particularly appropriate for calculating the differential capacitance of super-capacitors containing ionic liquids.[28,29] In this paper, we extend these techniques to efficiently simulate two infinite charged metal slabs inside an electrolyte solution (see Fig. 1).

Consider first an ion of charge q_i at position $\boldsymbol{r}_i = (x_i, y_i, z_i)$ in the region $z > 0$ in front of an infinite *grounded* metal slab located at $z = 0$ (see Fig. 2). To account for the periodic boundary condition of the simulation cell, the charge is periodically replicated in x and y directions with periodicity L_{xy}. The electrostatic potential at position $\boldsymbol{r} = (x, y, z)$, satisfies the Poisson equation

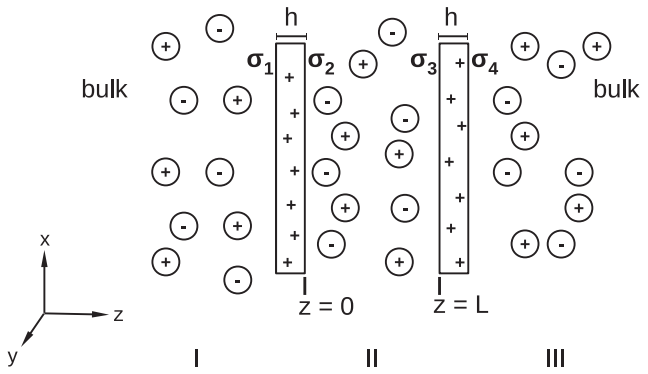

FIG. 1. Two metal slabs of width h and surface area L_{xy}^2 separated by a distance L inside an electrolyte solution.

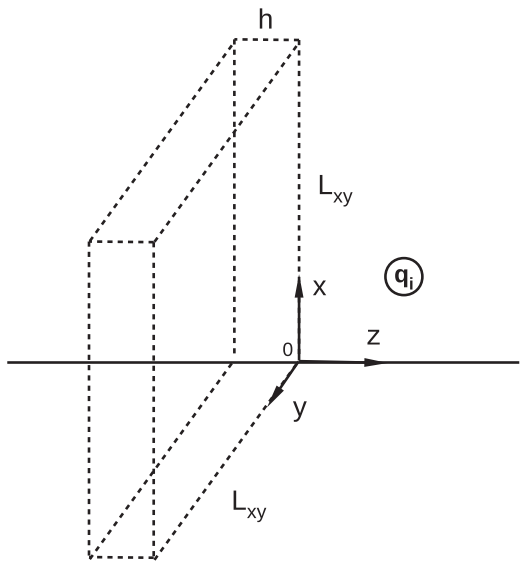

FIG. 2. Ion of charge q_i in the region $z > 0$ in front of a grounded metal slab of width h with its right face located at $z = 0$. The ion is replicated in x and y directions with periodicity L_{xy}.

$$\nabla^2 G(\boldsymbol{r};\boldsymbol{r}_i) = -\frac{4\pi q_i}{\epsilon_w} \sum_{m_x,m_y=-\infty}^{\infty} \delta(\boldsymbol{r} - \boldsymbol{r}_i + m_x L_{xy}\hat{\boldsymbol{x}} + m_y L_{xy}\hat{\boldsymbol{y}}), \quad (1)$$

where $m_{x,y}$ are integers and ϵ_ω is the dielectric constant of water. The periodic delta function can be expressed using a Fourier transform, and the Poisson equation can be solved analytically (see the supplementary material for details). The Green function is found to be

$$G(\boldsymbol{r};\boldsymbol{r}_i) = \frac{2\pi q_i}{\epsilon_\omega L_{xy}^2} \sum_{\boldsymbol{m}=-\infty}^{\infty} \frac{1}{k}\left(e^{-k|z-z_i|} - e^{-k(z+z_i)}\right) \times \cos\left[\frac{2\pi m_x}{L_{xy}}(x - x_i) + \frac{2\pi m_y}{L_{xy}}(y - y_i)\right], \quad (2)$$

where $k = 2\pi\sqrt{m_x^2/L_{xy}^2 + m_y^2/L_{xy}^2}$. In this calculation, we assumed that the metal slab was grounded. This means that as an ion and its replicas move, the surface charge distribution on the grounded metal slab changes in such a way as to keep the electrostatic potential of the slab constant. This excess charge is provided by the battery (or ground) to which the slab is connected. Furthermore, since the electric field inside a conductor must vanish, the induced charge must be distributed on the right-hand face of the slab in such a way as to precisely cancel the electric field produced by the ion in the interior of the slab. What happens if the slab is not connected to the battery? In this case, there is no source for the extra charge. Instead, the electronic charge inside the slab must reorganize itself in such a way as to cancel the electric field produced by the outside ion in the interior of the slab. Using the uniqueness property of the Laplace equation, we know that if we obtain a solution that satisfies all the boundary conditions, it must then be unique. Consider the solution for a grounded metal slab given by $G(\boldsymbol{r};\boldsymbol{r}_i)$. We know that this solution leads to the induced surface charge that is nonuniformly

distributed over the surface area L_{xy}^2 but which sums up precisely to $-q_i$. This excess charge is provided by the battery. In the case when there is no battery, there is no source for the extra charge. Therefore, we must add a countercharge to cancel the induced charge while keeping the electric field in the interior of the metal slab at zero. This can be done by placing a charge $q_i/2$ uniformly distributed over the area L_{xy}^2 on the face of the slab located at $z = 0$ and charge $q_i/2$ over the face located at $z = -h$. The electrostatic potential produced by the ion placed in front of a *neutral*, *ungrounded*, metal slab can then be expressed as the sum of $G(\boldsymbol{r}; \boldsymbol{r}_i)$ and a linear potential produced by the countercharge uniformly distributed on the two faces of the slab. Since this construction satisfies the Laplace equation with all the boundary conditions, we know that it must be the unique solution.

With the insights gained from the study of a single slab, we can now consider an electrolyte containing two parallel metal slabs, each of width h and separated by a face-to-face distance L (see Fig. 1). Again, we start by first considering *grounded* metal slabs. The ion q_i can be located in one of the three regions: I, II, and III (see Fig. 1). If the ion is either in region I or III, the Green function in Eq. (2) can be easily modified to the new geometry by simply shifting the origin of the coordinate system. Therefore, if the ion is in region I, the Green function is

$$G_I(\boldsymbol{r}; \boldsymbol{r}_i) = \frac{2\pi q_i}{\epsilon_\omega L_{xy}^2} \sum_{\boldsymbol{m}=-\infty}^{\infty} \frac{1}{k}\left(e^{-k|z-z_i|} - e^{k(z+z_i+2h)}\right) \times \cos\left[\frac{2\pi m_x}{L_{xy}}(x-x_i) + \frac{2\pi m_y}{L_{xy}}(y-y_i)\right]. \tag{3}$$

If the ion is region III, we find

$$G_{III}(\boldsymbol{r}; \boldsymbol{r}_i) = \frac{2\pi q_i}{\epsilon_\omega L_{xy}^2} \sum_{\boldsymbol{m}=-\infty}^{\infty} \frac{1}{k}\left(e^{-k|z-z_i|} - e^{-k(z+z_i-2L-2h)}\right) \times \cos\left[\frac{2\pi m_x}{L_{xy}}(x-x_i) + \frac{2\pi m_y}{L_{xy}}(y-y_i)\right]. \tag{4}$$

On the other hand, if the ion is located inside region II—between the two *grounded* metal slabs—the Green function for this situation was derived in Ref. 28 and is given by

$$G_{II}(\boldsymbol{r}; \boldsymbol{r}_i) = \frac{2\pi q_i}{\epsilon_\omega L_{xy}^2} \sum_{\boldsymbol{m}'=-\infty}^{\infty} \frac{1}{k(1-e^{-2kL})} \times \left[e^{-k|z-z_i|} - e^{-k(z+z_i)} - e^{-2kL}e^{k(z+z_i)} + e^{-2kL}e^{k|z-z_i|}\right] \times \cos\left[\frac{2\pi m_x}{L_{xy}}(x-x_i) + \frac{2\pi m_y}{L_{xy}}(y-y_i)\right]. \tag{5}$$

We note that an ion inside region I induces a charge $-q_i$ on the left face of the left slab, while the right face of this slab remains neutral. This charge is *nonuniformly* distributed over the surface area of the slab, L_{xy}^2, inside the simulation box. The charge comes from the battery to which the slab is connected to keep it at a fixed potential. If the ion is located in region III, the charge $-q_i$ will be induced on the right face of the right slab, while its left face remains neutral. Finally, if the ion is located at position z_i, in between the two slabs (region II), it will induce charge $-q_i(L - z_i)/L$ on the right face of the left slab and charge $-q_i z_i/L$ on the left face of the right slab.[27] The Green functions can be separated into the direct Coulomb interaction G^0 and the polarization contribution $\tilde{G}_j$ so that $G_j = G^0 + \tilde{G}_j$, where j specifies the region. The direct Coulomb interaction energy can then be easily calculated using a modified 3D Ewald summation[30] (see the discussion in the supplementary material).

The Green functions presented above are for metal slabs, the potentials of which are fixed by an external source, i.e., battery. As the position of the ion changes, the surface charge changes as well, so as to keep the electrostatic slab potential constant. If we are interested in studying neutral slabs, the net amount of charge on each slab must remain zero, independent of the position of the ion. This means that an additional surface charge must be added/subtracted to compensate for the induced charge sourced by the battery—if we want to use the Green functions derived above. The extra charge must be placed on the four faces of the slabs in such a way as to leave the electric field inside each slab equal to zero. The procedure is similar to the one presented earlier for a single metal slab.

We start by labeling the surfaces of the two slabs 1, 2, 3, and 4 from the left to right in Fig. 1. The left slab is designated as "*l*" and the right one as "*r*." If slabs are grounded, the ion q_i induces surface charge on the slabs. In the case of neutral slabs, this charge must be canceled by the added surface charges, σ_1, σ_2, σ_3, and σ_4, on the respective slab faces in order to use the Green functions given by Eqs. (3)–(5). Recall that the induced charge distributes itself in such a way as to exactly cancel the ionic electric field inside the conductor. The neutralizing surface charge, therefore, must also be arranged in a way as to preserve the zero electric field inside the two conductors as well as to neutralize completely the induced charge. We define σ_l and σ_r as the total additional surface charge on the left and right slabs, needed to neutralize the induced charge. This charge is *opposite* of the induced charge that is drawn to the slab when it is grounded. If the ion is located in region I, then

$$\begin{aligned} \sigma_l &= \frac{q_i}{L_{xy}^2}, \\ \sigma_r &= 0. \end{aligned} \tag{6}$$

If the ion is in region III, then

$$\begin{aligned} \sigma_l &= 0, \\ \sigma_r &= \frac{q_i}{L_{xy}^2}. \end{aligned} \tag{7}$$

If the ion is in region II at position z_i, then surface charge is induced on both slabs,[27]

$$\begin{aligned} \sigma_l &= \frac{q_i}{L_{xy}^2}\frac{(L-z_i)}{L}, \\ \sigma_r &= \frac{q_i}{L_{xy}^2}\frac{z_i}{L}. \end{aligned} \tag{8}$$

Furthermore, the condition of zero electric field inside conductors requires that

$$\sigma_1 + \sigma_2 = \sigma_l, \tag{9}$$

$$\sigma_3 + \sigma_4 = \sigma_r, \tag{10}$$

$$\sigma_1 = \sigma_4, \tag{11}$$

$$\sigma_2 = -\sigma_3. \tag{12}$$

Solving these equations for an ion located in one of the three regions, we obtain the additional neutralizing charge that must be placed on each surface in order to be able to use the Green functions calculated for the grounded slabs,

$$q_i \text{ in region I} \begin{cases} \sigma_1 &= \sigma_4 = +\dfrac{q_i}{2L_{xy}^2}, \\ \sigma_2 &= -\sigma_3 = +\dfrac{q_i}{2L_{xy}^2}, \end{cases}$$

$$q_i \text{ in region II} \begin{cases} \sigma_1 &= \sigma_4 = +\dfrac{q_i}{2L_{xy}^2}, \\ \sigma_2 &= -\sigma_3 = +\dfrac{q_i}{2L_{xy}^2}\left(1 - \dfrac{2z_i}{L}\right), \end{cases}$$

$$q_i \text{ in region III} \begin{cases} \sigma_1 &= \sigma_4 = +\dfrac{q_i}{2L_{xy}^2}, \\ \sigma_2 &= -\sigma_3 = -\dfrac{q_i}{2L_{xy}^2}. \end{cases}$$

The electrostatic potential Φ produced by the neutralizing charge must be added to the Green functions calculated with the Dirichlet boundary condition to obtain the total electrostatic potential for neutral metal slabs. The potential must be symmetric under the exchange of source and the observation point and must be continuous across the surfaces (see the supplementary material for details). Performing the calculations, we find, for the ion of charge q_i located in region I,

$$\Phi_I(\boldsymbol{r};\boldsymbol{r}_i) = \begin{cases} \dfrac{2\pi q_i}{\epsilon_\omega L_{xy}^2}\left(z + z_i + 2h + \dfrac{L}{2}\right) & \text{for } z < -h \\ -\dfrac{2\pi q_i}{\epsilon_\omega L_{xy}^2}\left(z - z_i - h - \dfrac{L}{2}\right) & \text{for } 0 > z > L \\ -\dfrac{2\pi q_i}{\epsilon_\omega L_{xy}^2}\left(z - z_i - 2h - \dfrac{L}{2}\right) & \text{for } z > L + h. \end{cases} \tag{13}$$

For the ion located in region II,

$$\Phi_{II}(\boldsymbol{r};\boldsymbol{r}_i) = \begin{cases} \dfrac{2\pi q_i}{\epsilon_\omega L_{xy}^2}\left(z - z_i + h + \dfrac{L}{2}\right) & \text{for } z < -h \\ -\dfrac{2\pi q_i}{\epsilon_\omega L_{xy}^2}\left(z + z_i - \dfrac{zz_i}{L/2} - \dfrac{L}{2}\right) & \text{for } 0 > z > L \\ -\dfrac{2\pi q_i}{\epsilon_\omega L_{xy}^2}\left(z - z_i - h - \dfrac{L}{2}\right) & \text{for } z > L + h. \end{cases} \tag{14}$$

Finally, for the ion located inside region III,

$$\Phi_{III}(\boldsymbol{r};\boldsymbol{r}_i) = \begin{cases} \dfrac{2\pi q_i}{\epsilon_\omega L_{xy}^2}\left(z - z_i + 2h + \dfrac{L}{2}\right) & \text{for } z < -h \\ \dfrac{2\pi q_i}{\epsilon_\omega L_{xy}^2}\left(z - z_i + h + \dfrac{L}{2}\right) & \text{for } 0 > z > L \\ -\dfrac{2\pi q_i}{\epsilon_\omega L_{xy}^2}\left(z + z_i - 2h - \dfrac{5L}{2}\right) & \text{for } z > L + h. \end{cases} \tag{15}$$

TABLE I. Electrostatic interaction potential between two ions in regions (i, j) for a system with two neutral metal slabs. We omit ($\boldsymbol{r}_j$; $\boldsymbol{r}_i$) from all expressions.

	I	II	III
I	$G_I + \Phi_I$	Φ_{II}	Φ_{III}
II	Φ_I	$G_{II} + \Phi_{II}$	Φ_{III}
III	Φ_I	Φ_{II}	$G_{III} + \Phi_{III}$

The electrostatic potential produced by the ion of charge q_i located inside the region j for a system containing two *neutral* metal slabs is

$$V_j(\boldsymbol{r};\boldsymbol{r}_i) = G_j(\boldsymbol{r};\boldsymbol{r}_i) + \Phi_j(\boldsymbol{r};\boldsymbol{r}_i), \tag{16}$$

where $G_j(\boldsymbol{r};\boldsymbol{r}_i)$ is the Green function calculated for the *grounded* metal slabs. The Green function contributes to the interaction potential only for ions located within the same region j. It does not act across the different regions. On the other hand, the potential $\Phi_j(\boldsymbol{r};\boldsymbol{r}_i)$ acts in *all* the regions. The electrostatic interaction potentials between charges located in regions I, II, and III for *neutral* metal slabs are summarized in Table I.

III. ENERGIES

The total electrostatic energy can be written as

$$\begin{aligned} U = &\sum_{j=1}^{N_I} q_j \left[\sum_{i\neq j}^{N_I} [G_I + \Phi_I] + \sum_{i=1}^{N_{II}} \Phi_{II} + \sum_{i=1}^{N_{III}} \Phi_{III} \right] \\ &+ \sum_{j=1}^{N_{II}} q_j \left[\sum_{i\neq j}^{N_{II}} [G_{II} + \Phi_{II}] + \sum_{i=1}^{N_{III}} \Phi_{III} \right] \\ &+ \sum_{j=1}^{N_{III}} q_j \sum_{i\neq j}^{N_{III}} [G_{III} + \Phi_{III}], \end{aligned} \tag{17}$$

where we have omitted ($\boldsymbol{r}_j$; $\boldsymbol{r}_i$) for clarity. We can split U into the contributions arising from the interaction of ions in the same region and across the different regions. The latter is controlled by the potential Φ. We find

$$U = U_{0_I} + U_{0_{II}} + U_{0_{III}} + U_{\tilde{G}_I} + U_{\tilde{G}_{II}} + U_{\tilde{G}_{III}} + U_{\Phi_I} + U_{\Phi_{II}} + U_{\Phi_{III}}, \tag{18}$$

where the direct Coulomb interaction within the region j, U_{0_j}, can be efficiently calculated using a modified 3D Ewald summation method.[30] $U_{\tilde{G}_j}$ accounts for the polarization contribution to the total energy within the region j. Finally, U_{Φ_j} is the energy due to the neutralizing charge that we added to keep the slabs neutral. This potential acts within the region j and across the different regions.

For region I, the polarization energy $U_{\tilde{G}_I}$ can be written as

$$U_{\tilde{G}_I} = -\frac{\pi}{\epsilon_\omega L_{xy}^2} \sum_{\boldsymbol{m}'=-\infty}^{\infty} \frac{1}{k}\left[f_{1,I}(\boldsymbol{m})^2 + f_{2,I}(\boldsymbol{m})^2\right] - \frac{2\pi}{\epsilon_\omega L_{xy}^2} Q_I M_I, \tag{19}$$

where $Q_I = \sum_{i=1}^{N_I} q_i$, $M_I = \sum_{i=1}^{N_I} q_i z_i$, and N_I is the number of particles inside region I. The number of integers (m_x, m_y) necessary to obtain

a converged energy depends on the lateral size of the simulation box L_{xy}. The choice of h is irrelevant since the potential is constant inside a slab so that we can set $h = 0$. The functions $f_{i,I}(\boldsymbol{m})$ are defined as

$$f_{1,I}(\boldsymbol{m}) = \sum_{i=1}^{N_I} q_i \cos\left[\frac{2\pi}{L_{xy}}(m_x x_i + m_y y_i)\right] e^{kz_i} \tag{20}$$

and

$$f_{2,I}(\boldsymbol{m}) = \sum_{i=1}^{N_I} q_i \sin\left[\frac{2\pi}{L_{xy}}(m_x x_i + m_y y_i)\right] e^{kz_i}. \tag{21}$$

For region II, we find

$$\begin{aligned} U_{\tilde{G}_{II}} = &-\frac{\pi}{\epsilon_\omega L_{xy}^2} \sum_{\boldsymbol{m}'=-\infty}^{\infty} \frac{1}{k(1-e^{-2kL})} \Big\{ f_{1,II}(\boldsymbol{m})^2 + f_{2,II}(\boldsymbol{m})^2 \\ &+ e^{-2kL}\left(f_{3,II}(\boldsymbol{m})^2 + f_{4,II}(\boldsymbol{m})^2\right) \\ &- 2e^{-2kL}\left[f_{3,II}(\boldsymbol{m}) f_{1,II}(\boldsymbol{m}) + f_{2,II}(\boldsymbol{m}) f_{4,II}(\boldsymbol{m})\right] \Big\} \\ &- \frac{2\pi}{\epsilon_\omega L_{xy}^2}\left(\frac{M_{II}^2}{L} - Q_{II} M_{II}\right), \end{aligned} \tag{22}$$

where $Q_{II} = \sum_{i=1}^{N_{II}} q_i$, $M_{II} = \sum_{i=1}^{N_{II}} q_i z_i$, and N_{II} is the number of particles in region II. The functions $f_{i,II}(\boldsymbol{m})$ are

$$f_{1,II}(\boldsymbol{m}) = \sum_{i=1}^{N_{II}} q_i \cos\left[\frac{2\pi}{L_{xy}}(m_x x_i + m_y y_i)\right] e^{-kz_i}, \tag{23}$$

$$f_{2,II}(\boldsymbol{m}) = \sum_{i=1}^{N_{II}} q_i \sin\left[\frac{2\pi}{L_{xy}}(m_x x_i + m_y y_i)\right] e^{-kz_i}, \tag{24}$$

$$f_{3,II}(\boldsymbol{m}) = \sum_{i=1}^{N_{II}} q_i \cos\left[\frac{2\pi}{L_{xy}}(m_x x_i + m_y y_i)\right] e^{kz_i}, \text{ and} \tag{25}$$

$$f_{4,II}(\boldsymbol{m}) = \sum_{i=1}^{N_{II}} q_i \sin\left[\frac{2\pi}{L_{xy}}(m_x x_i + m_y y_i)\right] e^{kz_i}. \tag{26}$$

For region III, the polarization contribution is

$$\begin{aligned} U_{\tilde{G}_{III}} = &-\frac{\pi}{\epsilon_\omega L_{xy}^2} \sum_{\boldsymbol{m}'=-\infty}^{\infty} \frac{1}{k}\left[f_{1,III}(\boldsymbol{m})^2 + f_{2,III}(\boldsymbol{m})^2\right] \\ &+ \frac{2\pi}{\epsilon_\omega L_{xy}^2}\left(Q_{III} M_{III} + Q_{III}^2 L\right), \end{aligned} \tag{27}$$

where $Q_{III} = \sum_{i=1}^{N_{III}} q_i$, $M_{III} = \sum_{i=1}^{N_{III}} q_i z_i$, and N_{III} is the number of particles in region III, and the functions $f_{i,III}(\boldsymbol{m})$ are

$$f_{1,III}(\boldsymbol{m}) = \sum_{i=1}^{N_{III}} q_i \cos\left[\frac{2\pi}{L_{xy}}(m_x x_i + m_y y_i)\right] e^{-k(z_i - L)} \tag{28}$$

and

$$f_{2,III}(\boldsymbol{m}) = \sum_{i=1}^{N_{III}} q_i \sin\left[\frac{2\pi}{L_{xy}}(m_x x_i + m_y y_i)\right] e^{-k(z_i - L)}. \tag{29}$$

The contributions U_{Φ_j} can be written as

$$U_{\Phi_I} = \frac{\pi}{\epsilon_\omega L_{xy}^2}\left[Q_t M_I + Q_I(M_I - M_{II} - M_{III}) + \frac{L}{2} Q_I Q_t\right], \tag{30}$$

$$\begin{aligned} U_{\Phi_{II}} = &\frac{\pi}{\epsilon_\omega L_{xy}^2}\left[M_{II}\left(Q_{III} - Q_I + \frac{2}{L} M_{II}\right)\right. \\ &\left. + Q_{II}\left(M_I - M_{III} - 2M_{II} + \frac{2}{L} Q_t\right)\right], \end{aligned} \tag{31}$$

and

$$\begin{aligned} U_{\Phi_{III}} = &\frac{\pi}{\epsilon_\omega L_{xy}^2}\left[M_{III}(-Q_I - Q_{II} - 2Q_{III})\right. \\ &\left. + Q_{III}\left[M_I + M_{II} + \frac{L}{2}(Q_I + Q_{II} + 5Q_{III})\right]\right], \end{aligned} \tag{32}$$

where $Q_t = Q_I + Q_{II} + Q_{III}$.

With the present method, we can model neutral slabs in an electrolyte solution. If slabs are non-neutral, the excess surface density σ_{s_1} and σ_{s_2} on each slab will lead to an additional external electrostatic potential that will act on the ions. This potential can be written as

$$\Phi_{ex}(z) = \begin{cases} \frac{2\pi}{\epsilon_\omega}\left[(\sigma_{s_1} + \sigma_{s_2})z + (\sigma_{s_1} - \sigma_{s_2})\frac{L}{2}\right] & \text{for } z < 0 \\ \frac{2\pi}{\epsilon_\omega}(\sigma_{s_2} - \sigma_{s_1})\left(z - \frac{L}{2}\right) & \text{for } 0 > z > L \\ -\frac{2\pi}{\epsilon_\omega}\left[(\sigma_{s_1} + \sigma_{s_2})(z - L) + (\sigma_{s_1} - \sigma_{s_2})\frac{L}{2}\right] & \text{for } z > L, \end{cases} \tag{33}$$

where we have set the width of slabs $h = 0$ and the zero of the potential at $z = L/2$. The excess surfaces charge will lead to an additional contribution to the total energy,

$$U_{ex} = \sum_{i=1}^{N} q_i \Phi_{ex}(z_i). \tag{34}$$

IV. MONTE CARLO SIMULATIONS

The Monte Carlo simulations are performed using the Metropolis algorithm in the *NVT* ensemble. Metal slabs are separated by a distance L and their width is set to $h = 0$, without any loss of generality. The electrolyte is confined within $L_z/4 \geq z \geq -L_z/4$. For $L_z > z > L_z/4$ and $-L_z/4 > z > -L_z$, there is a vacuum region. The lateral extent of the simulation cell is $L_z = 3L_{xy}$ so that $L_z \gg L$. The vacuum region is included in order to use the recently developed[30] efficient modified 3D Ewald summation method to account for the direct Coulomb interaction. The ions have radius $r_c = 2$ Å, while water is modeled as a uniform medium of dielectric constant ϵ_ω. The phase space is sampled using short and long displacement moves.[31] The Bjerrum length is $\lambda_B = q^2\beta/\epsilon_\omega$, where β is the inverse thermal energy and q is the proton charge. We set $\lambda_B = 7.2$ Å, the typical value for water at room temperature. The ionic density profiles are obtained using 5×10^4 uncorrelated samples.

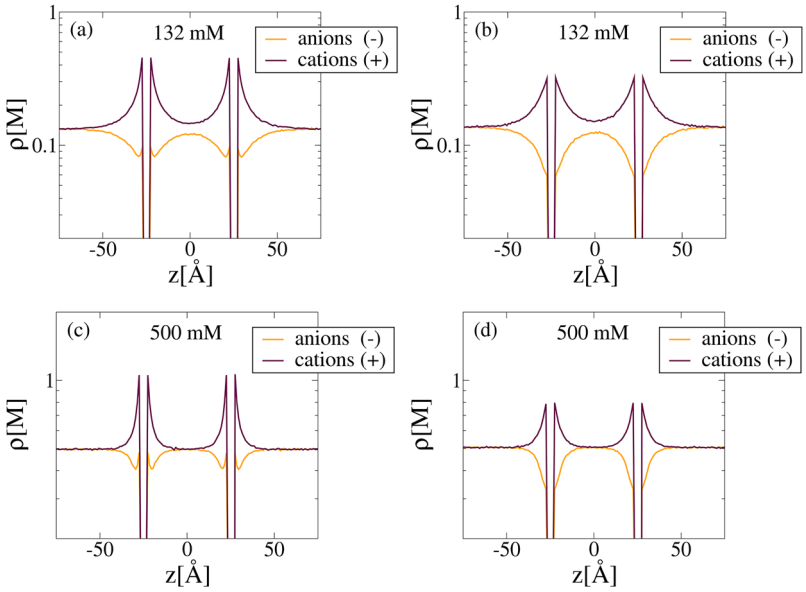

FIG. 3. Density profiles of cations and anions for the 1:1 electrolyte. [(a) and (c)] The slabs are metal. [(b) and (d)] The slabs are nonpolar charged hard walls. In both cases, the surface charge density is $\sigma_{s_1} = \sigma_{s_2} = \sigma_s = -0.04$ C/m^2. The separation between the slabs is L = 50 Å, and the slab thickness is h = 0.

Note that $f_j(\boldsymbol{m})$ functions, M_j, and Q_j must be updated for each particle move—there is, however, no need to recalculate the whole sum, but only the contribution that depends on the position of the particle that is being moved. This makes the energy update very efficient. An essential characteristic of the new algorithm is that the components of the total energy are decoupled both from each other and between different regions (with the exception of the terms U_{Φ_j} and U_{ex} that come from the surface potentials). Finally, we also note that parity of functions $f_j(\boldsymbol{m})$ allows us to rewrite the sums in a way that requires only half of the **m** terms in the energy calculations.

In Figs. 3 and 4, we compare the density profiles of 1:1 and 3:1 electrolytes for metal and nonmetal negatively charged slabs separated by the distance L = 50 Å. The region outside the slabs is taken to be sufficiently large to allow the ionic density profiles to relax to their bulk values. The results for nonpolar surfaces were taken from the previous work.[32] We see a significant effect of polarizability on the ionic distributions. This is particularly dramatic in the case of electrolytes with multivalent ions. In this case, the large valence of cations leads to strong charge-image attraction, which results in a remarkable adsorption of cations to the surface. In Fig. 4, we see that the buildup of counterions near the surface is so large as to drive the

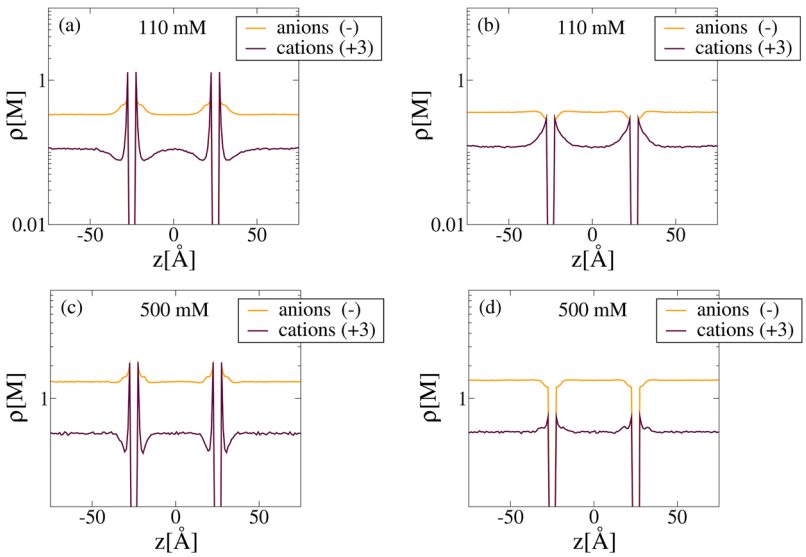

FIG. 4. Density profiles of cations and anions for the 3:1 electrolyte. [(a) and (c)] The slabs are metal. [(b) and (d)] The slabs are charged nonpolar hard walls. In both cases, the surfaces charge density is $\sigma_{s_1} = \sigma_{s_2} = \sigma_s = -0.04$ C/m^2. The separation between the surfaces is L = 50 Å, and the slab thickness is h = 0. Note a very strong adsorption of multivalent counterions to the charged metal slabs. Furthermore, even the monovalent co-ions (anions) become adsorbed to the like-charged metal slabs.

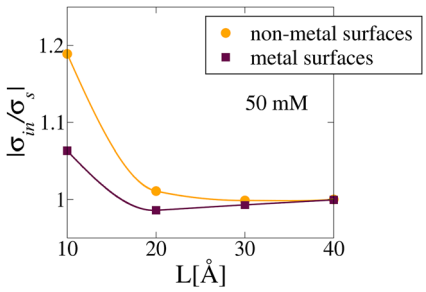

FIG. 5. Deviation from charge neutrality in between the slabs as a function of slab separation. Charge neutral state, $\sigma_{in}/\sigma_s = 1$, is obtained at large separations. The bulk 3:1 salt concentration is 50 mM, while the surface charge density is $\sigma_s = -0.08$ C/m^2. The symbols are the simulation data, while the lines are the interpolation curves.

adsorption of co-ions to a like-charged surface. Strong adsorption of counterions can lead to the reversal of the electrophoretic mobility of metal nanoparticles.

In Ref. 32, the breakdown of charge neutrality between charged nonmetal surfaces was studied using MC simulations. For two like-charged slabs with the total surface charge density σ_s each, the charge neutral state is defined as $\sigma_{in} = \sigma_s$, where σ_{in} is the total ionic charge density in between the two slabs,

$$\sigma_{in} = \frac{\langle Q \rangle}{L_{xy}^2}, \tag{35}$$

where $\langle Q \rangle$ is the average total charge in between the two slabs. In Fig. 5, we compare the ratio $|\sigma_{in}/\sigma_s|$ for metal and non-metal slabs. We observe that the polarizability of surfaces diminishes the charge neutrality violation at short slab separations.

V. CONCLUSION

We have presented a new method to efficiently simulate ionic distribution around two infinite charged metal slabs immersed in an electrolyte solution. The approach is based on the exact solution of the Poisson equation that allows us to calculate the interaction potential between two charges in the presence of neutral metal slabs. In this paper, we have considered two metal slabs; however, our approach can be easily extended to an arbitrary number of slabs. We find that the ionic density profiles are significantly modified by the slab polarizability. In the case of 3:1 electrolytes, we find the effect of polarizability to be so strong as to lead to adsorption of co-ions to a like-charged surface. The new simulation approach may be useful for studying anomalous screening in the presence of surfaces[33] as well as order–disorder transition in confined ionic liquids. Finally, we note that the method developed here can now be combined with a modified Derjaguin approximation[5] to calculate the force between two spherical metal nano-particles. This will be a subject of the future work.

SUPPLEMENTARY MATERIAL

See the supplementary material for a detailed derivation of the Green function for a periodic charge in front of a grounded metal slab and a derivation of the potential produced by the neutralizing surface charge.

ACKNOWLEDGMENTS

This work was partially supported by the CNPq, FAPERGS, and INCT-FCx and by the US-AFOSR under Grant No. FA9550-16-1-0280. M.G. thanks FAPESP under Grant No. 2019/06088-3.

DATA AVAILABILITY

The data that support the findings of this study are available within the article (and its supplementary material).

REFERENCES

[1] M.-C. Daniel and D. Astruc, Chem. Rev. **104**, 293 (2004).
[2] A. Bakhshandeh, Chem. Phys. **513**, 195 (2018).
[3] B. Petersen, R. Roa, J. Dzubiella, and M. Kanduč, Soft Matter **14**, 4053 (2018).
[4] P. S. Ghosh, C.-K. Kim, G. Han, N. S. Forbes, and V. M. Rotello, ACS Nano **2**, 2213 (2008).
[5] A. P. dos Santos and Y. Levin, Phys. Rev. Lett. **122**, 248005 (2019).
[6] N. L. Rosi, D. A. G. C. S. Thaxton, A. K. R. Lytton-Jean, and M. S. H. C. A. Mirkin, Science **312**, 1027 (2006).
[7] D. A. Giljohann, D. S. Seferos, W. L. Daniel, M. D. Massich, P. C. Patel, and C. A. Mirkin, Angew. Chem., Int. Ed. **49**, 3280 (2010).
[8] D. Boda, D. Gillespie, W. Nonner, D. Henderson, and B. Eisenberg, Phys. Rev. E **69**, 046702 (2004).
[9] T. P. Doerr and Y. Yu, Phys. Rev. E **73**, 061902 (2006).
[10] S. Tyagi, M. Süzen, M. Sega, M. Barbosa, S. S. Kantorovich, and C. Holm, J. Chem. Phys. **132**, 154112 (2010).
[11] V. Jadhao, F. J. Solis, and M. O. de la Cruz, Phys. Rev. Lett. **109**, 223905 (2012).
[12] K. Barros and E. Luijten, Phys. Rev. Lett. **113**, 017801 (2014).
[13] L. Šamaj and E. Trizac, Europhys. Lett. **100**, 56005 (2012).
[14] L. Šamaj and E. Trizac, Contrib. Plasma Phys. **52**, 53 (2012).
[15] J. W. Zwanikken and M. Olvera de la Cruz, Proc. Natl. Acad. Sci. USA **110**, 5301 (2013).
[16] Y. Nakayama and D. Andelman, J. Chem. Phys. **142**, 044706 (2015).
[17] T. Markovich, D. Andelman, and H. Orland, J. Chem. Phys. **145**, 134704 (2016).
[18] L. Šamaj, A. P. dos Santos, Y. Levin, and E. Trizac, Soft Matter **12**, 8768 (2016).
[19] A. P. dos Santos and R. R. Netz, J. Chem. Phys. **148**, 164103 (2018).
[20] T. D. Nguyen and M. Olvera de la Cruz, ACS Nano **13**, 9298 (2019).
[21] J. I. Siepmann and M. Sprik, J. Chem. Phys. **102**, 511 (1995).
[22] S. Tyagi, A. Arnold, and C. Holm, J. Chem. Phys. **127**, 154723 (2007).
[23] A. P. dos Santos and Y. Levin, J. Chem. Phys. **142**, 194104 (2015).
[24] A. Arnold, K. Breitsprecher, F. Fahrenberger, S. Kesselheim, O. Lenz, and C. Holm, Entropy **15**, 4569 (2013).
[25] H. Heinz, T.-J. Lin, R. Kishore Mishra, and F. S. Emami, Langmuir **29**, 1754 (2013).
[26] I. L. Geada, H. Ramezani-Dakhel, T. Jamil, M. Sulpizi, and H. Heinz, Nat. Commun. **9**, 716 (2018).
[27] M. Girotto, A. P. dos Santos, and Y. Levin, J. Chem. Phys. **147**, 074109 (2017).

[28]A. P. dos Santos, M. Girotto, and Y. Levin, J. Chem. Phys. **147**, 184105 (2017).
[29]M. Girotto, R. M. Malossi, A. P. dos Santos, and Y. Levin, J. Chem. Phys. **148**, 193829 (2018).
[30]A. P. dos Santos, M. Girotto, and Y. Levin, J. Chem. Phys. **144**, 144103 (2016).
[31]D. Frenkel and B. Smit, *Understanding Molecular Simulation: From Algorithms to Applications* (Elsevier Science, 2001).
[32]T. Colla, M. Girotto, A. P. dos Santos, and Y. Levin, J. Chem. Phys. **145**, 094704 (2016).
[33]A. M. Smith, A. A. Lee, and S. Perkin, J. Phys. Chem. Lett. **7**, 2157 (2016).